A Macroscopic Model for Multi-Modal Traffic Flow in Urban Networks

Agatha Joumaa, Paola Goatin, Giovanni de Nunzio

A Macroscopic Model for Multi-Modal Traffic Flow in Urban Networks

Agatha Joumaa[1,2], Paola Goatin[2], Giovanni De Nunzio[1]

***Abstract*— This paper presents a macroscopic multi-class traffic flow model on road networks that accounts for an arbitrary number of vehicle classes with different free flow speeds. A comparison of the Eulerian and Lagrangian formulations is proposed, with the introduction of a new Courant-Friedrichs-Lewy condition. In particular, the $\mathbf{L}^1$-error and the computational times are used to compare the performance of the two formulations and show that the Eulerian formulation outperforms the Lagrangian. The paper then extends the Eulerian formulation to traffic networks, providing a general implementation of the dynamics at junctions. We finally simulate the effect of traffic measures and policies, such as route guidance and modal shift, on total travel time and network throughput, which shows that the proposed multi-class model correctly depicts the interactions among classes and it can be used to model such behaviors in complex networks.**

***Index Terms*— Multi-class macroscopic traffic flow models, Hyperbolic systems of conservation laws, Eulerian and Lagrangian formulations, Finite volume schemes.**

I. INTRODUCTION

The rapid evolution of people mobility, driven by technological advancements and changing employment patterns, combined with the increasing use of shared and soft modes of transportation, has made the modeling of traffic flow on roads and networks a complex and challenging task. Traditional approaches based on static demand data are unable to capture the complex interactions between vehicles of different types, and do not reflect the evolving mobility landscape. To address this issue, a macroscopic dynamical model for multi-class traffic flow is proposed in this paper.

In recent years, there has been a significant amount of research conducted with the primary objective of describing the interactions that occur between various types of vehicles on the road using macroscopic multi-class traffic flow models. This includes cars and trucks (e.g. [1], [2]), cars and motorcycles (e.g. [3], [4]), and even the coexistence of human-driven and autonomous vehicles on shared roads (e.g. [5], [6]). The multi-class Lighthill-Whitham-Richards (LWR) model is one of the simplest continuum traffic flow models in the literature. It has been widely used in traffic engineering, transportation planning, and operations research, in either its Eulerian or Lagrangian formulations. The Eulerian description has been used for example to capture overtaking and creeping effects as shown by [3], mixed traffic and varying number of lanes [7] and passenger cars and buses in an urban area for a bus-rapid transit system [8]. The Lagrangian formulation has been extensively used in modeling mixed bicycle-car traffic as in [9], mixed traffic that includes trucks [10], and powered two-wheelers [11]. While the difference between the two formulations has been addressed by [12], a clear comparison of the two approaches in terms of the trade-off between accuracy and computational time has not been discussed yet to our knowledge. In this paper, we give a detailed analysis of the two descriptions and we show that the Eulerian formulation is better adapted for fast and accurate simulations of generic multi-class traffic flows on road networks. Therefore, the Eulerian formulation appears more suitable for use in large-scale networks and for solving optimal multi-modal traffic management problems. To this aim, we also introduce a generic description of multi-class traffic dynamics at road junctions in Eulerian coordinates. The extension to network has been addressed in the literature both in the Eulerian framework as in [13], [14], [15] and in Lagrangian coordinates (see [12], [16]), the latter leading to cumbersome manipulations.

Aiming at testing the model capabilities to capture multi-class traffic dynamics, we run simulations on a simple toy network of thirteen roads with both urban and peri-urban characteristics, showing the interaction between three classes of vehicles representing small and fast vehicles such as cars, big and slow vehicles such as trucks, and small and slow vehicles such as bikes. We note that, in this study, classes are characterized by their different free-flow speeds.

The contributions of this work are therefore threefold. First, we give a detailed analysis of the well-posedness of finite volume approximations for the multi-class LWR model both in Eulerian and Lagrangian coordinates, providing a refined Courant-Friedrichs-Lewy (CFL) stability condition for the Lagrangian formulation ensuring positivity of solutions (the usual CFL condition assumes only one vehicle class). Second, we compare the Eulerian and Lagrangian formulations of the multi-class LWR model in terms of the trade-off between accuracy and computational time. Our results show that the Eulerian formulation outperforms the Lagrangian one. Finally, we present a network generalization in Eulerian coordinates, including inflow and outflow boundary conditions at origin and destination nodes, respectively. We also provide a numerical study involving three different types of vehicles, where we investigate the sensitivity of the proposed model to two application scenarios: vehicles rerouting and modal shift.

The remainder of the paper is organized as follows. In Section II, we present the multi-class LWR model in both Eulerian and Lagrangian coordinates, and compare them. In

[1]A. Joumaa and G. De Nunzio are with IFP Energies nouvelles, Rond-point de l'échangeur de Solaize, BP 3, 69360 Solaize, France {agatha.joumaa, giovanni.de-nunzio}@ifpen.fr

[2]A. Joumaa and P. Goatin are with Université Côte d'Azur, Inria, CNRS, LJAD, 2004, route des Lucioles - BP 93 06902 Sophia Antipolis Cedex, FRANCE {agatha.joumaa, paola.goatin}@inria.fr

Section III, we extend the Eulerian formulation to networks, and construct solutions for general merge and diverge junctions. We also include the rigorous treatment of inflow and outflow boundary conditions at origin and destination nodes. In Section IV, we provide numerical results for a simple network, where we compute total travel time (TTT) and network throughput (NT) of the whole population. Finally, we conclude the paper in Section V.

II. Methodology

In this section, we describe and compare the Eulerian and Lagrangian formulations of the macroscopic multi-class traffic flow model we consider in this work.

A. Eulerian formulation

We consider the $N \times N$ system of conservation laws [1]

$$\boldsymbol{\rho}_t + \mathbf{F}(\boldsymbol{\rho})_x = 0, \tag{1}$$

where $\boldsymbol{\rho} = (\rho^1, \dots, \rho^N)^T$ is the multi-class density of vehicles with $c = 1, 2, \dots, N$, denoting the vehicle class, and $\mathbf{F}(\boldsymbol{\rho}) = \psi(r)(V_1\rho^1, \dots, V_N\rho^N)^T$ is the flux function. Above, the overall density is denoted as $r = \sum_{c=1}^N \rho^c$, the class specific free-flow speeds verify $V_1 > \ldots > V_N$, and ψ is a decreasing function such that $\psi(0) = 1$ and $\psi(1) = 0$, meaning that we set the maximal density to 1 without loss of generality. We also set the class specific speed function $v_c(r) := V_c\,\psi(r)$. System (1) is then defined on the simplex

$$\mathcal{S}_E = \left\{ \boldsymbol{\rho} \in \mathbb{R}^N \colon \rho^c \geq 0 \text{ and } \sum_{c=1}^N \rho^c \leq 1 \right\}.$$

Following [17], [18], [5], we approximate system (1) by finite volume schemes of the form

$$\rho_j^{c,k+1} = \rho_j^{c,k} - \frac{\Delta t}{\Delta x}\left[F_{j+1/2}^{c,k} - F_{j-1/2}^{c,k}\right], \tag{2}$$

where $j \in \mathbb{Z}$ is the space index, $k \in \mathbb{N}$ is the time index, and

$$F_{j+1/2}^{c,k} := \frac{\rho_j^{c,k}}{r_j^k} \min\left\{D^c(r_j^k), S^c(r_{j+1}^k)\right\} \tag{3}$$

is the Godunov numerical flux in its supply-demand formulation (see [5, Eq. (4)]). Above, D^c and S^c are respectively the demand and supply functions of the total density relatively to the c-th class speed defined by setting $Q^c(r) := rv_c(r)$, $r_{cr}^c := \arg\max_r Q^c(r)$ and

$$D^c(r) := Q^c(\min\{r, r_{cr}^c\}), \tag{4}$$

$$S^c(r) := Q^c(\max\{r, r_{cr}^c\}). \tag{5}$$

The scheme (2)-(5) satisfies the following $\mathbf{L}^\infty$ estimates (see [6, Lemma 2.3] for a similar result.).

Lemma 1: (Domain invariance) Under the CFL condition

$$V_1\left(\|\psi\|_\infty + N\|\psi'\|_\infty\right)\Delta t \leq \Delta x, \tag{6}$$

for any initial data $\boldsymbol{\rho}_0 \in \mathcal{S}_E$ the approximate solutions computed by the Godunov scheme (3), satisfy the following uniform bounds:

$$\boldsymbol{\rho}_j^k \in \mathcal{S}_E \quad \forall j \in \mathbb{Z},\ k \in \mathbb{N}.$$

Proof: Assuming that $\rho_j^{c,k} \geq 0$ for $c = 1, \dots, N$ and $\sum_{c=1}^N \rho_j^{c,k} \leq 1$ for all $j \in \mathbb{Z}$, we show that the same holds for $\boldsymbol{\rho}_j^{k+1}$. For positivity:

$$\begin{aligned}
\rho_j^{c,k+1} &\geq \rho_j^c - \frac{\Delta t}{\Delta x}\frac{\rho_j^c}{r_j}\min\left\{D^c(r_j), S^c(r_{j+1})\right\} \\
&\geq \rho_j^c - \frac{\Delta t}{\Delta x}\frac{\rho_j^c}{r_j}Q^c(\min\{r_j, r_{j,cr}\}) \\
&\geq \rho_j^c - \frac{\Delta t}{\Delta x}\frac{\rho_j^c}{r_j}r_j v_c(\min\{r_j, r_{j,cr}\}) \\
&= \rho_j^c\left(1 - \frac{\Delta t}{\Delta x}v_c(\min\{r_j, r_{j,cr}\})\right) \geq 0
\end{aligned}$$

under the CFL condition (6). On the other side

$$\begin{aligned}
\sum_{c=1}^N \rho_j^{c,k+1} &\leq \sum_{c=1}^N \rho_j^c + \frac{\Delta t}{\Delta x}\sum_{c=1}^N \frac{\rho_{j-1}^c}{r_{j-1}}\min\left\{D^c(r_{j-1}), S^c(r_j)\right\} \\
&\leq \sum_{c=1}^N \rho_j^c + \frac{\Delta t}{\Delta x}\sum_{c=1}^N \frac{\rho_{j-1}^c}{r_{j-1}}S^c(r_j).
\end{aligned}$$

Setting $\phi(\boldsymbol{\rho}) := \sum_{c=1}^N \rho^c + \frac{\Delta t}{\Delta x}\sum_{c=1}^N \frac{\rho_{j-1}^c}{r_{j-1}}S^c(r)$, we get $\phi(\boldsymbol{\rho}) = 1$ if $\sum_{c=1}^N \rho^c = 1$ and

$$\frac{\partial \phi}{\partial \rho^\ell}(\boldsymbol{\rho}) \geq 1 - \frac{\Delta t}{\Delta x}\sum_{c=1}^N ||(S^c)'||_\infty \geq 0,$$

where we used that $0 \leq \frac{\rho_{j-1}^c}{r_{j-1}} \leq 1$ and (6). Hence $\phi(\boldsymbol{\rho}) \leq 1$ for all $\boldsymbol{\rho} \in \mathcal{S}_E$. ∎

B. Lagrangian formulation

To rewrite equation (1) in Lagrangian coordinates, we introduce the class-specific spacing as

$$s^c = \frac{1}{\rho^c}, \qquad c = 1, \dots, N, \tag{7}$$

Replacing (7) and the Lagrangian time derivative defined as $\frac{D}{Dt} = \frac{\partial}{\partial t} + v\frac{\partial}{\partial x}$ in (1), we get the Lagrangian formulation of the multi-class LWR model:

$$\frac{Ds^c}{Dt} + \frac{\partial \tilde{v}_c}{\partial n} = 0, \tag{8}$$

where $\tilde{v}_c = \tilde{v}_c(\mathbf{s}) := v_c\left(\sum_{\ell=1}^N 1/s^\ell\right)$.

System (8) is then defined on the set

$$\mathcal{S}_L = \left\{ \mathbf{s} = (s^1, \dots, s^N) \in \mathbb{R}^N \colon s^c \geq 0 \text{ and } \sum_{c=1}^N \frac{1}{s^c} \leq 1 \right\}.$$

Following [16], we can approximate (8) using an upwind discretization method. The spacing s^c is approximated by constant values between n^c and $n^c + \Delta n$ and it is updated at every time step Δt^k. Since $\tilde{v}_c$ is increasing in s^c, the characteristic speed is always nonnegative, reflecting the anisotropic behavior:

$$s_j^{c,k+1} = s_j^{c,k} + \frac{\Delta t^k}{\Delta n}(v_{c,j+1}^k - v_{c,j}^k), \tag{9}$$

where $v^k_{c,j} = \tilde{v}_c(\mathbf{s}^k_j) := v_c\left(\sum_{\ell=1}^N 1/s^{\ell,k}(x^{c,k}_j)\right)$ and

$$x^{c,k}_j = x^{c,k-1}_j + \Delta t^{k-1}\, v^{k-1}_{c,j}$$

are the position of the cell interfaces at time t^k. Notice that, unlike (2), it is not possible to take a uniform time discretization step, but Δt^k is updated at each iteration. Indeed, $\nabla\tilde{v}_c(\mathbf{s}) = -v_c'\left(\sum_{\ell=1}^N 1/s^\ell\right)\left(1/(s^1)^2,\dots,1/(s^N)^2\right)^T$ and therefore

$$\|\nabla\tilde{v}_c(\mathbf{s})\|_\infty \le \frac{N\,\|v_c'\|_\infty}{\min_{c=1,\dots,N}\|s^c\|^2_\infty}.$$

The following Lemma provides a necessary CFL condition for the Lagrangian scheme (9).

Lemma 2: (Positivity) Under the CFL condition

$$\Delta t^k\, N\|v_c'\|_\infty \frac{\max_{c,j}\left|s^{c,k}_j\right|}{\min_{c,j}\left|s^{c,k}_j\right|^3} \le \Delta n, \tag{10}$$

for any initial data $\mathbf{s}_0 \in \mathcal{S}_L$ the approximate solutions computed by the scheme (9) satisfy $\mathbf{s}^k_j \ge 0 \quad \forall j \in \mathbb{Z},\ k \in \mathbb{N}$.

Proof: We proceed by induction: assuming that $s^{c,k}_j \ge 0$ for $c = 1,\dots,N$ for all $j \in \mathbb{Z}$, we show that the same holds for s^{k+1}_j. We focus on one s^c component, the procedure being similar for others. We compute

$$\begin{aligned}
s^{c,k+1}_j &= s^{c,k}_j + \frac{\Delta t}{\Delta n}(v^k_{c,j+1} - v^k_{c,j}) \\
&= s^{c,k}_j + \frac{\Delta t}{\Delta n}\nabla\tilde{v}_c(\xi^k_{j+1/2})\cdot\left(\mathbf{s}^k_{j+1} - \mathbf{s}^k_j\right) \\
&\ge s^{c,k}_j - s^{c,k}_j\frac{\Delta t^k}{\Delta n}\nabla\tilde{v}_c(\xi^k_{j+1/2})\cdot\mathbf{s}^k_j\frac{1}{s^{c,k}_j} \\
&\ge s^{c,k}_j\left(1 - \frac{\Delta t^k}{\Delta n}\|\nabla\tilde{v}_c\|_\infty\|\mathbf{s}^k_j\|_\infty\frac{1}{s^{c,k}_j}\right) \\
&\ge s^{c,k}_j\left(1 - \frac{\Delta t^k}{\Delta n}N\|v_c'\|_\infty\frac{\max_{c,j}\left|s^{c,k}_j\right|}{\min_{c,j}\left|s^{c,k}_j\right|^3}\right) \ge 0
\end{aligned}$$

by (10). Above, $\xi^k_{j+1/2} = \theta\mathbf{s}^k_j + (1-\theta)\mathbf{s}^k_{j+1}$, $\exists\theta \in [0,1]$. ■

C. Comparison between Eulerian and Lagrangian

For the purpose of our work, we compare the computational efficiency of the Eulerian and Lagrangian formulations. To this end, we consider a Riemann problem for two classes of vehicles, with initial densities

$$\rho^1(0,x) = \begin{cases} 0.5, & x < 0, \\ 0, & x > 0, \end{cases} \qquad \rho^2(0,x) = \begin{cases} 0, & x < 0, \\ 0.5, & x > 0, \end{cases}$$

and with maximal speeds $V_1 = 1$ and $V_2 = 0.6$, respectively for class 1 and 2. For each formulation, we compute the $\mathbf{L^1}$-error of approximate solutions with respect to a numerical reference solution, which is given by

$$Err(\Delta x_m) := \Delta x \sum_j \left|\bar{\rho}_j - \rho_{\ell_j}\right|$$

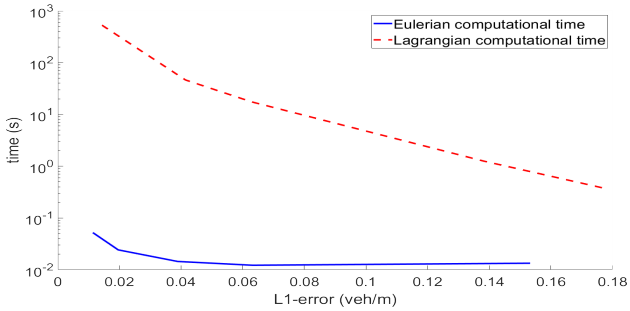

Fig. 1: Computational time Vs $\mathbf{L^1}$ error

where $\bar{\rho}_j$, $j \in \mathbb{Z}$, is the reference solution computed by Godunov method on a fine mesh with $\Delta x = 10^{-5}$ and ρ_ℓ, $\ell \in \mathbb{Z}$, is the approximate solution computed on a coarser grid $\Delta x_m = m\Delta x$, $m \in \mathbb{N}$.

We note that, to compute the error for the Lagrangian approximations, one has to transform the computed spacing back to the corresponding density and to match the moving Lagrangian space grid with the fixed Eulerian mesh.

To evaluate the efficiency of the two approaches, we compare the computational times needed for both methods to attain the same $\mathbf{L^1}$-error range, by varying the parameters Δn (for the Lagrangian) and Δx_m (for the Eulerian). Figure 1 illustrates the computational time vs the $\mathbf{L^1}$ error for both methods, showing that the Eulerian approximation outperforms the Lagrangian approach. The parameters used in the simulations are $\Delta n = \{0.001, 0.005, 0.01, 0.05, 0.1\}$ and $\Delta x_m = \{0.0025, 0.005, 0.0125, 0.025, 0.1\}$ pairwise, with higher values leading to larger error.

It is therefore clear that the Eulerian setting offers several advantages, such as a much lower computational time for a prescribed accuracy goal, as well as the possibility to fix a-priori the time step Δt and to avoid dealing with moving space grids, which complicate the Lagrangian model extension to road networks. In the sequel of the paper, we will then work in the Eulerian framework.

III. Extension to Networks

We consider road networks represented by graphs of directed arcs connected at nodes [19]. While traffic flow on edges can be described by the model introduced in the previous section, modeling traffic dynamics at junctions is the major element of the network extension. In the CTM initial study [20], junctions that were taken into consideration were only simple merges and diverges. In the present work, we detail the procedure for the 1×1 (one incoming and one outgoing road), $M \times 1$ ($M > 1$ incoming roads and one outgoing road) and $1 \times M$ (one incoming road and M outgoing roads) types of junctions. Junctions with additional incoming and outgoing links can typically be reduced to a mixture of the last two fundamental junction types. We will explain how the flux over the node can be calculated in a multi-class kinematic wave model, given the traffic status at the incoming and outgoing roads.

In Eulerian formulation, junction models rely on the

minimum supply-demand method. More precisely, the flux through the junction results from the demand of the incoming link(s) and the supply of the outgoing link(s).

A. Solutions at junctions for N classes of vehicles

In the following, we give the solutions of the Riemann Problem for simple junctions [19], i.e. for the cases 1×1, $M \times 1$, $1 \times M$ for N classes of vehicles. The demand and supply are given by equations (4) and (5), but they may be different on each road, thus depending on the index $i = 1, \dots, M+1$.

1) Solution to 1×1 *junction:* For the 1×1 junction, we adapt (3) by setting:

$$\hat{\gamma}_1^c = \hat{\gamma}_2^c = \frac{\rho_1^c}{r_1} \min\left\{D_1^c(r_1), S_2^c(r_2)\right\}, \qquad c = 1, \dots, N.$$

2) Solution to $M \times 1$ *(merge) junction:* A class specific priority vector $P^c = (p_1^c, \dots, p_M^c) \in \mathbb{R}^M$, $p_i^c \geq 0$, $\sum_{i=1}^M p_i^c = 1$ is required, so that $\hat{\gamma}_i^c = p_i^c\, \hat{\gamma}_{M+1}^c$ for $i = 1, \dots, M$. The corresponding fluxes are:

$$\hat{\gamma}_i^c = \frac{\rho_i^c}{r_i} \min\Big\{D_i^c(r_i), \max\left\{p_i^c S_{M+1}^c(r_{M+1}), S_{M+1}^c(r_{M+1}) - \sum_{j \neq i} D_j^c(r_j)\right\}\Big\}, \quad (11)$$

$$\hat{\gamma}_{M+1}^c = \sum_{i=1}^M \hat{\gamma}_i^c,$$

for $c = 1, \dots, N$.

3) Solution for $1 \times M$ *(diverge) junction:* The class specific distribution matrix A^c takes the form

$$A^c = \left(\alpha_2^c, \dots, \alpha_{M+1}^c\right)^T,$$

where $\alpha_i^c \geq 0$, $\sum_{i=2}^{M+1} \alpha_i^c = 1$, indicate the percentage of vehicles of class c going from road 1 to road i. Then, the fluxes at the junction are computed as:

$$\hat{\gamma}_i^c = \alpha_i^c \hat{\gamma}_1^c, \quad i = 2, \dots, M+1,$$

where

$$\hat{\gamma}_1^c = \frac{\rho_1^c}{r_1} \min\left\{D_1^c(r_1), \frac{S_2^c(r_2)}{\alpha_2^c}, \dots, \frac{S_{M+1}^c(r_{M+1})}{\alpha_{M+1}^c}\right\},$$

for $c = 1, \dots, N$.

Note that, if traffic does not get fully congested, the above FIFO rule gives similar results as a non-FIFO formulation.

B. Boundary conditions

Let $F_{in} = (F_{in}^1, \dots, F_{in}^N)^T$ and $F_{out} = (F_{out}^1, \dots, F_{out}^N)^T$ be respectively the inflow boundary conditions at an origin node and the outflow boundary condition at a destination node (where we assume $F_{in}^c, F_{out}^c \geq 0$ for all $c = 1, \dots, N$).

From (3), (11), we can define

$$\hat{\gamma}_{in}^c = \min\left\{F_{in}^c, \max\left\{\frac{1}{N} S^c(r_1), S^c(r_1) - \sum_{g \neq c} F_{in}^g\right\}\right\},$$

$$\hat{\gamma}_{out}^c = \frac{\rho_J^c}{r_J} \min\left\{D^c(r_J), F_{out}^c\right\},$$

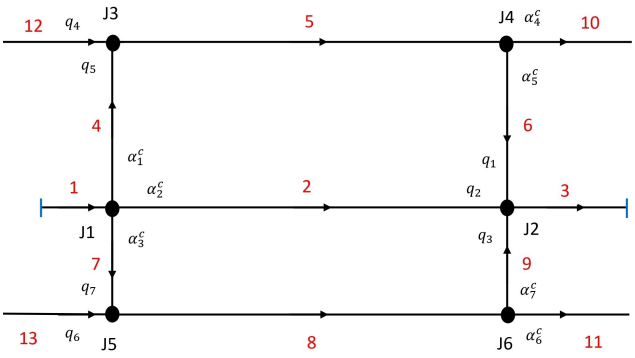

Fig. 2: Schematic representation of the considered network

where r_1 and r_J are the density values respectively in the first and last cell of the concerned roads.

IV. Simulation results

In the following tests, we consider an elementary network of 13 roads and 6 junctions, consisting of a main road and two additional routes available as secondary itineraries in case of heavy traffic, see Fig. 2. We assume the presence of three classes of vehicles: cars, trucks and bikes, with $V_{cars} > V_{trucks} > V_{bikes}$, in consistency with our hypothesis. Cars can circulate on the whole network with a speed of 70 km/h on the main path (roads 1-2-3) and 50 km/h on the secondary paths (roads 4-5-6 and roads 7-8-9). On the contrary, trucks are only allowed on the main path (roads 1-2-3) with a speed of 50 km/h. Finally, bikes can only travel on roads 12-5-10 and 13-8-11 with a speed of 15 Km/h. Road 1 measures 100 m, roads 2, 5 and 8 have a length of 1000 m, 300 m for roads 4 and 6 and finally 200 m for roads 3, 7, 9, 10, 11, 12 and 13. We consider a uniform grid with step size $\Delta x = 5$ m and the time is sampled with steps $\Delta t = 0.25$ s. At the merge junction J2, we take $q_1 = q_3 = 0.2$ and consequently $q_2 = 0.6$ for all classes, meaning that vehicles coming from the main road have priority over those coming from the lateral ones. At the merge junctions J3 and J5, we give priority to the bikes i.e. roads 12 and 13 with $q_4 = q_6 = 0.8$. On the diverge junctions J1, J4 and J6, the distribution coefficients for trucks are $\alpha_2^{\text{trucks}} = 1$ and 0 everywhere else, since trucks are only allowed to circulate on the main road. Similarly for bikes, since those that enter from road 12 can only leave from road 10 and those that enter from road 13 go to road 11, we set $\alpha_4^{\text{bikes}} = \alpha_6^{\text{bikes}} = 1$ and 0 everywhere else. As for cars, we set $\alpha_4^{\text{cars}}, \alpha_5^{\text{cars}}, \alpha_6^{\text{cars}}, \alpha_7^{\text{cars}}$ equal to 0.5, meaning that cars do not have a preference at the diverge junctions J4 and J6. Finally, the simulated inflow at the network boundaries is set as the maximal possible inflow on the time interval $[0, T]$, ensuring that all vehicles can enter in free flow, and it is set equal to 0 on $(T, T_f]$, where $T_f > T > 0$ are prescribed time horizons.

In order to assess the proposed model sensitivity to complex interactions among the different classes of vehicles, we propose to evaluate the overall traffic performance by means of two metrics: total travel time (TTT) and network

throughput (NT). The TTT of a given class c, i.e. the space and time integral of the corresponding density, is defined as:

$$\text{TTT}(\rho^c) = \Delta t \Delta x \sum_{k=0}^{T_f} \sum_{i} \sum_{j=0}^{N_i} \rho_{i,j}^{c,k}$$

where N_i is the number of cells in the road segment i, $i \in [1, 13]$ the road index, and T_f the final simulation time. The NT of class c, i.e the total number of vehicles of that class leaving the network (time integral of the total outflow of the network), is defined as:

$$\text{NT}(\rho^c) = \sum_{k=0}^{T_f} \sum_{i} \hat{\gamma}_{out,i}^{c,k}$$

where $i \in \{3, 10, 11\}$ is the road index. By linearity, the global TTT and NT are given by the sum of the corresponding class specific quantities:

$$\text{TTT}(r) = \sum_{c=1}^{N} TTT(\rho^c), \qquad \text{NT}(r) = \sum_{c=1}^{N} NT(\rho^c).$$

In the following experiments, NT is calculated for $T_f = T = 500\,\text{s}$ to be able to capture the number of vehicles leaving the network when the inflow is stopped, while TTT is calculated for $T_f = 1100\,\text{s}$ so that T_f is large enough for all the vehicles to leave the network. The boundary outflow $\hat{\gamma}_{out}^c$ on roads 10 and 11 is set to maximal flow to allow vehicles to leave the network undisturbed, while it is set to half the maximal flow at the end of road 3 to induce congestion on the network, as though a traffic light was regulating outgoing traffic. Finally, in order to have a meaningful comparison, we normalize both metrics by dividing them by the maximum value they achieved for each class during the experiment.

A. Experiment 1 (Rerouting)

The first experiment consists in evaluating the effect of progressively rerouting cars at J1 from the main path to the secondary paths. The idea is that rerouting the cars will alleviate congestion on the main road, thus improving travel time for trucks. However, rerouted cars will have to take a longer path at lower speed and to share the secondary roads with bikes, which may have a negative impact on the overall network performance. In this experiment, the network is initially empty and the boundary conditions at the entry and exit roads are given by III-B with an inflow of cars, trucks and bikes equal to their maximal flow, that is $V_c/4$, and F_{out}^c is the maximum supply obtained for a total density $r = 0$. We let the distribution coefficient of the cars at J1 be variable, i.e. $\alpha_1^{\text{cars}} = \alpha_3^{\text{cars}} = \alpha \in [0, 0.5]$ towards the lateral roads 4 and 7, which implies $\alpha_2^{\text{cars}} = 1 - 2\alpha$ on road 2.
Figure 3 shows that with the increase of α (thus the percentage of cars taking the secondary paths), the global TTT first decreases, reaching a minimum value around $\alpha = 0.4$, but then increases again, due to congestion forming on roads 4 and 7. It is clear that the TTT of trucks decreases when α increases, since they can move faster on the main road if cars reroute to the lateral ones. On the contrary, the TTT for bikes increases when cars leave the main road.

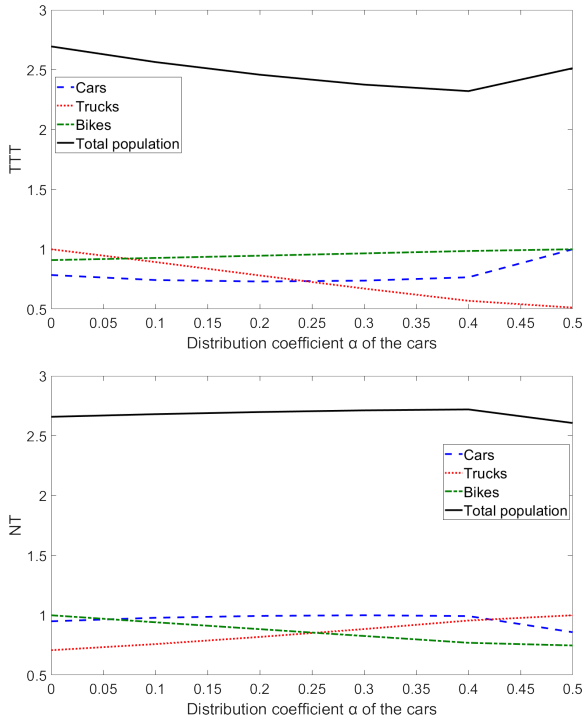

Fig. 3: Experiment 1 - TTT (top) and NT (bottom) on the whole network for each of the three vehicle classes and for the total population as a function of the distribution coefficient $\alpha \in [0, 0.5]$ at the diverge junction J1.

Figure 3 (bottom) shows the NT of the three classes and the total traffic, which attains its maximum for $\alpha = 0.4$, because when the network is less congested, more vehicles are able to leave. Clearly, the NT of the 3 classes has a completely opposite behavior of their TTT.

B. Experiment 2 (Modal shift)

The second experiment aims to evaluate the impact of modal shift on the overall network performance. In particular, we investigate the benefits of progressively shifting cars flow towards bikes flow, thus simulating the effect of public policies incentivizing the uptake of soft transportation modes. In this experiment, we use the exact same initial conditions and parameters as the first one except for the inflow on roads 1, 12 and 13. The proportion between bikes and cars is given by a parameter $\theta \in [0, 1]$, as we set a global inflow

$$F_{in,cb} = \frac{V_{\text{bikes}}}{2} = \frac{15}{3.6 \times 2} \text{ veh/s}$$

and

$$F_{in,cars} = (1 - \theta) F_{in,cb}, \quad F_{in,trucks} = \frac{V_{\text{trucks}}}{4} - F_{in,cb}$$

on road 1, and $F_{in,bikes} = \frac{\theta}{2} F_{in,cb}$ on roads 12 and 13.
We set $\alpha_1^{\text{cars}} = \alpha_3^{\text{cars}} = 0.4$, because this was the optimal value for the overall performance in the previous experiment. We notice that the global TTT in Figure 4 (top) reaches a

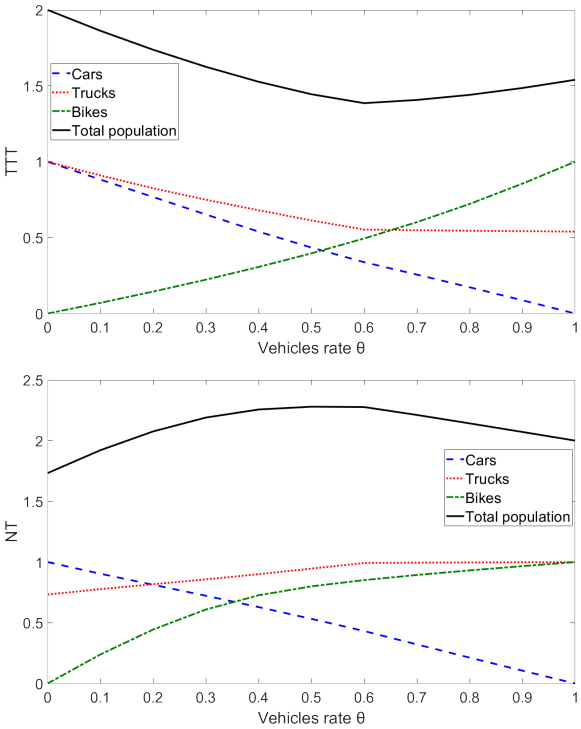

Fig. 4: Experiment 2 - TTT (top) and NT (bottom) on the whole network for each of the three vehicle classes and for the total population as a function of the bike vs cars percentage $\theta \in [0, 1]$ at inflow boundary conditions.

minimum for $\theta = 0.6$, then increases again for higher values of θ. It is clear that for $\theta = 0$, i.e when there are no bikes, the TTT of cars is maximal and conversely when $\theta = 1$, i.e when there are no cars, the TTT of bikes is maximal. The TTT of trucks experiences a rapid decrease until θ reaches 0.6, and subsequently, it exhibits a more gradual decrease. In Figure 4 (bottom), we can see that the total number of vehicles leaving the network is maximized between $\theta = 0.5$ and $\theta = 0.6$. As expected, this is consistent with the results of the TTT and it means that if 60% of drivers choose to use bikes instead of cars, it could reduce congestion in the network and improve travel times.

V. CONCLUSION

In this paper, we have presented a multi-class macroscopic traffic flow model that is able to deal with an arbitrary number of vehicle classes. We showed by comparison that, for our purposes, working in Eulerian coordinates is more convenient than the Lagrangian setting, especially in terms of computational time. Additionally, the presented model has been extended to networks, and solutions for different types of junctions have been provided. The numerical experiments conducted in this study reveal that the model is able to capture the complex interactions among different classes of vehicles. The total travel time and the network throughput can be affected by various factors such as the distribution coefficient of cars (α) at diverge junctions and the rate of cars and bikes entering the network (θ). The results show that, for specific values of α and θ within the variation intervals, the total travel time and the network throughput are optimized. This is very promising because it shows that the model does not lead to trivial solutions, and it can be used in closed-loop optimization frameworks.

REFERENCES

[1] S. Benzoni-Gavage and R. M. Colombo, "An n-populations model for traffic flow," European J. Appl. Math., vol. 14, no. 5, pp. 587–612, 2003.

[2] J. W. C. van Lint, S. P. Hoogendoorn, and M. Schreuder, "Fastlane: New multiclass first-order traffic flow model," Transportation Research Record, vol. 2088, no. 1, pp. 177–187, 2008.

[3] S. Fan and D. B. Work, "A heterogeneous multiclass traffic flow model with creeping," SIAM J. Appl. Math., vol. 75, no. 2, pp. 813–835, 2015.

[4] S. Gashaw, P. Goatin, and J. Härri, "Modeling and analysis of mixed flow of cars and powered two wheelers," Transportation Research Part C: Emerging Technologies, vol. 89, pp. 148–167, 2018.

[5] M. W. Levin and S. D. Boyles, "A multiclass cell transmission model for shared human and autonomous vehicle roads," Transportation Research Part C: Emerging Technologies, vol. 62, pp. 103–116, 2016.

[6] F. A. Chiarello and P. Goatin, "Non-local multi-class traffic flow models," Netw. Heterog. Media, vol. 14, no. 2, pp. 371–387, 2019.

[7] K. Tiaprasert, Y. Zhang, C. Aswakul, J. Jiao, and X. Ye, "Closed-form multiclass cell transmission model enhanced with overtaking, lane-changing, and first-in first-out properties," Transportation Research Part C: Emerging Technologies, vol. 85, pp. 86–110, 2017.

[8] H. Liu, J. Wang, K. Wijayaratna, V. V. Dixit, and S. T. Waller, "Integrating the bus vehicle class into the cell transmission model," IEEE Transactions on Intelligent Transportation Systems, vol. 16, no. 5, pp. 2620–2630, 2015.

[9] M.-J. Wierbos, V. Knoop, F. Hänseler, and S. Hoogendoorn, "A macroscopic flow model for mixed bicycle–car traffic," Transportmetrica A: Transport Science, vol. 17, no. 3, pp. 340–355, 2021.

[10] F. van Wageningen-Kessels, H. Van Lint, S. P. Hoogendoorn, and K. Vuik, "Lagrangian formulation of multiclass kinematic wave model," Transportation Research Record, vol. 2188, no. 1, pp. 29–36, 2010.

[11] S. Gashaw, J. Härri, and P. Goatin, "Lagrangian formulation for mixed traffic flow including two-wheelers," in 2018 21st International Conference on Intelligent Transportation Systems (ITSC), pp. 1956–1961, IEEE, 2018.

[12] F. van Wageningen-Kessels, Multi-class continuum traffic flow models: analysis and simulation methods. PhD thesis, Delft University of Technology, 2013.

[13] P. Goatin, S. Göttlich, and O. Kolb, "Speed limit and ramp meter control for traffic flow networks," Engineering Optimization, vol. 48, no. 7, pp. 1121–1144, 2016.

[14] C. M. Tampère, R. Corthout, D. Cattrysse, and L. H. Immers, "A generic class of first order node models for dynamic macroscopic simulation of traffic flows," Transportation Research Part B: Methodological, vol. 45, no. 1, pp. 289–309, 2011.

[15] G. Flötteröd and J. Rohde, "Operational macroscopic modeling of complex urban road intersections," Transportation Research Part B: Methodological, vol. 45, no. 6, pp. 903–922, 2011.

[16] L. Leclercq, J. Laval, E. Chevallier, et al., "The lagrangian coordinates and what it means for first order traffic flow models," Transportation and traffic theory, pp. 735–753, 2007.

[17] R. Bürger, A. García, K. H. Karlsen, and J. D. Towers, "A family of numerical schemes for kinematic flows with discontinuous flux," J. Engrg. Math., vol. 60, no. 3-4, pp. 387–425, 2008.

[18] M. Briani and E. Cristiani, "An easy-to-use algorithm for simulating traffic flow on networks: theoretical study," Netw. Heterog. Media, vol. 9, no. 3, pp. 519–552, 2014.

[19] M. Garavello, K. Han, and B. Piccoli, Models for vehicular traffic on networks, vol. 9. American Institute of Mathematical Sciences Springfield, MO, USA, 2016.

[20] C. F. Daganzo, "The cell transmission model, part II: network traffic," Transportation Research Part B: Methodological, vol. 29, no. 2, pp. 79–93, 1995.